Journal of Power Sources 196 (2011) 2283–2288

Contents lists available at ScienceDirect

Journal of Power Sources

journal homepage: www.elsevier.com/locate/jpowsour

Short communication

Novel lithium titanate hydrate nanotubes with outstanding rate capabilities and long cycle life

Rui Xu[a], Junrong Li[b], Ao Tan[a], Zilong Tang[a,*], Zhongtai Zhang[a]

[a] State Key Laboratory of New Ceramics and Fine Processing, Department of Materials Science and Engineering, Tsinghua University, Beijing 100084, China
[b] China Astronaut Center, Beijing 100084, China

ARTICLE INFO

Article history:
Received 13 May 2010
Received in revised form
12 September 2010
Accepted 14 September 2010
Available online 22 September 2010

Keywords:
Li-ion batteries
Anode
Cathode
Rate capability
Cycling life

ABSTRACT

Novel lithium titanate hydrate nanotubes for lithium ion batteries have been easily prepared via a hydrothermal method. This material demonstrates high energy density, outstanding rate capabilities and a very long cycle life comparable to those of supercapacitors. At a rate equivalent to a 10-min total charge/discharge, the as-prepared lithium titanate hydrate nanotubes exhibit a life of over 5000 charge/discharge cycles while still retaining up to 86.3% of its original capacity. The abilities of lithium titanate hydrate nanotubes to fully charge within minutes for thousands of times and still retain a large capacity may find promising applications in hybrid and plug-in hybrid electric vehicles.

1. Introduction

Lithium ion batteries that can perform high power operations and have long cycle lives are greatly needed for hybrid and plug-in hybrid electric vehicles. Among the potential electrode materials for lithium ion batteries, nanostructured materials, especially one-dimensional nanostructured materials as have drawn much research interest due to their outstanding properties superior to the corresponding bulk counterparts [1–3]. Among these one-dimensional nanostructured materials, the spinel lithium titanate ($Li_4Ti_5O_{12}$) nanotube, known as the "zero-strain" lithium insertion host, undergoes little structural change during charge/discharge cycling, and its spinel framework provides three-dimensional network channels for fast Li-ion diffusion [4]. Hence the spinel $Li_4Ti_5O_{12}$, theoretically, could exhibit a long cycle life, excellent lithium ion intercalation/deintercalation reversibility and promising high-rate capabilities [5–9]. However, despite the above structure advantages for spinel $Li_4Ti_5O_{12}$, the material's lithium-ion conductivity and electron conductivity are quite low [10]. This disadvantage results in lower experimental values of $Li_4Ti_5O_{12}$'s electrochemical properties, which are not nearly as good as the theoretical ones. In order to increase its electron conductivity, a number of strategies have been applied to $Li_4Ti_5O_{12}$, such as incorporating a conducting second phase such as Ag [11], Cu [12], CuO_x [6] or $Li_2CuTi_3O_8$ [13], doping with alien-valent metal ions such as Ta^{5+} [14] or Al^{3+} [15], synthesizing nano-sized [16,17] $Li_4Ti_5O_{12}$, and heat treating $Li_4Ti_5O_{12}$ under low oxygen partial pressure atmosphere [18].

In this study, we focus on the synthesis, structural characterization and electrochemical investigation of lithium titanate hydrate nanotubes ($Li_{1.81}H_{0.19}Ti_2O_5{\cdot}xH_2O$). This material, on which few reports have been found, has demonstrated extraordinary rate capabilities, a much longer cycle life and larger capacities than $Li_4Ti_5O_{12}$ nanotubes due to its containing of crystal water, higher lithium-ion conductivity, pseudocapacitive feature of lithium intercalation and larger specific surface area. In addition, lithium titanate hydrate nanotubes can be obtained via a much easier preparation method.

2. Experimental

2.1. Preparation of materials

In a typical lithium titanate hydrate preparation procedure, hydrogen titanate nanotubes precursors were first prepared by adding industrial anatase TiO_2 powders to concentrated NaOH solution (10 M) and ultrasonically agitated at the power of 0.5 W cm^{-2} for 1 h. Then the suspension was stirred for 4 h before being transferred into a Teflon-lined stainless steel autoclave and maintained at 150 °C for 24 h for hydrothermal reaction. After the

* Corresponding author. Tel.: +86 10 62783685; fax: +86 10 62771160.
E-mail address: tzl@tsinghua.edu.cn (Z. Tang).

0378-7753/$ – see front matter © 2010 Elsevier B.V. All rights reserved.
doi:10.1016/j.jpowsour.2010.09.023

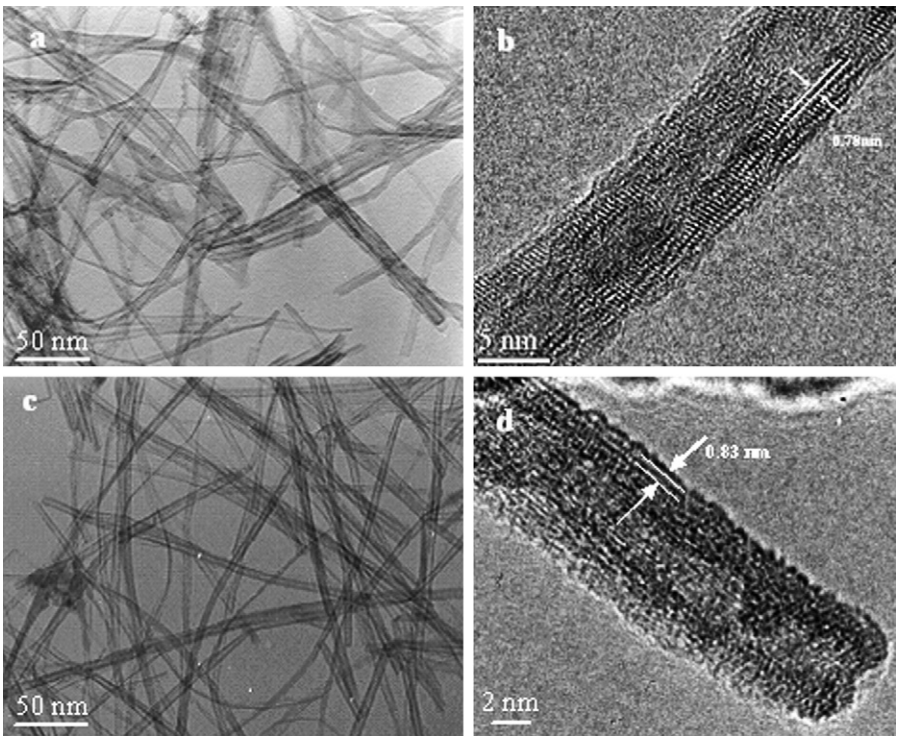

Fig. 1. Representative microstructures of hydrogen titanate precursors (a and b) and lithium titanate hydrate nanotubes (c and d). (a and c) Transmission electron microscopy image showing a nanotube length of hundreds of nanometers. (b and d) High-resolution transmission electron microscopy image showing an inter-layer spacing of around 0.78 nm for hydrogen titanate precursors and 0.83 nm for lithium titanate hydrate nanotubes, and a multi-wall nanotube outer diameter of 9 nm for both materials.

treatment, the white precipitate was acid-washed with 0.2 M HNO_3 or HCl solution at pH 3 for 1 h, then filtered and thoroughly washed. The hydrogen titanate prepared by previous work [19] was believed to be $H_2Ti_3O_7$ [20–22] or $H_2Ti_2O_4(OH)_2$ [23], a family of layered hydrogen titanate with a general formula of $H_2Ti_nO_{2n+1}\cdot H_2O$ [24], or orthorhombic $H_xTi_{2-x/4}\square_{x/4}O_4\cdot H_2O$ ($x \approx 0.7$, $\square$ = vacancy) with the lepidocrocite-type structure [25].

To prepare lithium titanate hydrate nanotubes, hydrogen titanate nanotubes were mixed with a 0.5 M LiOH aqueous solution and stirred vigorously for 1 h. The resulting suspension underwent a hydrothermal reaction at 150 °C for 40 h. The resulting white precipitate was filtered, washed and dried. The as-prepared lithium titanate hydrate nanotubes have a layer structure with crystal water incorporated in the interlayer, similar to $RuO_2\cdot H_2O$ [26] and $Na_{0.3}MnCoO_{1.95}\cdot nH_2O$ [27]. Bach et al. suggested that this crystal water ensures the elasticity of the layer structure and promotes the cycle life [28]. Meanwhile the nanotube structure limits Li^+ diffusion in the solid state phase within the small radius direction and thus promotes the efficiency of lithium ion migration. Hence lithium titanate hydrate nanotubes have a large reversible capacity, remarkable rate capabilities and outstanding cycling stablility. This material, with a main discharge voltage of about 1.5–1.6 V versus lithium, could be a promising anode material for many lithium ion batteries using high voltage materials such as $LiCoO_2$ and $LiMnO_2$ as their cathodes, and meanwhile could also be a cathode material working with graphite or silicon as anodes. On the other hand, spinel $Li_4Ti_5O_{12}$ nanotubes were also prepared, using the method introduced by Li [17], for comparison with the electrochemical properties of lithium titanate hydrate nanotubes.

2.2. Characterization of material

The morphologies of the as-prepared samples were characterized by transmission electron microscopy (TEM) performed on a JEOL JEM-200CX. High-resolution transmission electron microscopy (HRTEM) was performed on a TECNAI F30 (Philips). Powder X-ray diffraction (XRD) was performed on a Rigaku D/max-RB diffractometer operating in transmission mode with Cu Kα radiation (λ = 1.5418 Å). Thermogravimetric-differential thermal analysis (TG-DTA) was performed on a SETARAM-TGA92 with a temperature range of room temperature to 600 °C. Infrared (IR) spectra were obtained on a PE-FTIP-Spectrum GX type Fourier transform infrared spectrometer. The BET specific surface area was measured using a Quantachrome NOVA 4000 system with the N_2 absorption–desorption method at liquid nitrogen temperature.

2.3. Electrochemical property test

To fabricate the cathodes for the battery test cells, the as-prepared lithium titanate hydrate nanotubes, Super P carbon black, and polyvinylidene fluoride (PVDF) binder were mixed homogeneously in a weight ratio of 80:10:10 in a N-methyl pyrrolidinone (NMP) solvent. The electrode films were fabricated using the doctor blade technique on carbon covered aluminum foil. The loading of active material was 1–2 mg cm^{-2}. The coin-type half cell (CR2032 size) consisted of this electrode, a lithium metal counter electrode, a microporous polyethylene separator, and electrolyte of 1 M solution of $LiPF_6$ in ethylene carbonate/dimethyl carbonate (EC/DMC) (1:1, vol%; Merck). The cell was constructed and handled in an Ar-filled vacuum glove box. The discharge/charge tests were carried out using a LAND Celltest 2001 A (Wuhan, China) system between 2.5 and 1.0 V. First the test cell was discharged for Li^+ ions to intercalate into the cathode, and then the test cell was charged and held at 2.5 V to fully charge before discharge. Cyclic voltammogram was recorded from 2.5 to 1.0 V at a scan rate of 0.05 mV s^{-1}. AC impedance was measured at 1.6 V in a frequency range 0.1–10^5 Hz, using IM6e electrochemical workstation (Germany).

3. Results and discussions

3.1. Characterization of materials

The transmission electron microscopy and high-resolution transmission electron microscopy images in Fig. 1 show the microstructures of hydrogen titanate precursors and lithium titanate hydrate nanotubes. The outer diameter of these nanotubes was about 9 nm, and their lengths were hundreds of nanometers. The microstructure of the two materials was similar with that of hydrogen titanate nanotubes [19–25,28,29] and spinel titanate nanotubes [17]. The high-resolution transmission electron microscopy microgram shows clearly the well-crystallized multi-wall nanotube of lithium titanate hydrate with an inter-shell spacing of around 0.83 nm, which was much larger than that in typical commercial layered transitional metal oxide lithium ion battery materials [28].

The as-prepared lithium titanate hydrate nanotubes and their precursor of hydrogen titanate nanotubes were examined via X-ray diffraction (shown in Fig. 2a and b). It was found that the formula of the precursors was $H_2Ti_2O_5{\cdot}xH_2O$ with orthorhombic lattice (JCPDS Card No. 47-0124), which exhibited features similar to $H_2Ti_3O_7$, $H_xTi_{2-x/4}\square_{x/4}O_4{\cdot}H_2O$ and other members of the hydrogen titanate family [24]. Fig. 2b shows X-ray diffraction profiles of as-prepared lithium titanate hydrate nanotubes. The diffraction peaks of these nanotubes were in accordance with $Li_{1.81}H_{0.19}Ti_2O_5{\cdot}xH_2O$ (orthorhombic phase, JCPDS Card No. 47-0123, $a = 1.666$, $b = 0.3797$, $c = 0.3007$ nm). To further confirm this result, a chemical analysis will be needed. It can be concluded that the lithium titanate hydrate nanotubes have similar structure as their precursors of hydrogen titanate nanotubes, which are constructed by wrapping a (1 0 0) plane, with axis parallel to [0 1 0] [30]. The calculated interlayer spacing of the $Li_{1.81}H_{0.19}Ti_2O_5{\cdot}xH_2O$ nanotubes was 0.833 nm, agreeing with that observed using high-resolution transmission electron microscopy.

Detailed thermogravimetric-differential thermal analysis in Fig. 2c shows a weight loss of around 15% for the as-prepared $Li_{1.81}H_{0.19}Ti_2O_5{\cdot}xH_2O$ nanotubes after heated from room temperature to 600 °C. The weight loss at temperatures lower than 100 °C was primarily attributed to the desorption of surface absorbed water. Weight loss at temperatures above 100 °C, about 12%, was mostly due to the loss of the crystal water in $Li_{1.81}H_{0.19}Ti_2O_5{\cdot}xH_2O$ and the dehydration of $Li_{1.81}H_{0.19}Ti_2O_5$. Thus the approximate composition of the prepared nanotubes can be calculated, which is $Li_{1.81}H_{0.19}Ti_2O_5{\cdot}1.2H_2O$. To further confirm this result, a chemical analysis may be needed.

Fig. 2d shows the infrared spectra pattern of lithium titanate hydrate nanotubes, suggesting possible existence of crystal water in the material. The sample was heated at 403 K for several hours to eliminate surface adsorption water just before the test. Small absorption bands of the nanotubes with centers located between 400 cm^{-1} and 900 cm^{-1} can be clearly observed. These absorption bands corresponded to the asymmetric stretching vibrations of the octahedral groups [TiO_6] lattice [31]. A broad peak at 3000–3700 cm^{-1}, which was centered at around 3200 cm^{-1}, was the stretching mode of crystal water, and a strong peak at 1600–1700 cm^{-1} was due to the bending mode of water. This result indicates that the as-prepared nanotubes contained crystal water, well supporting the X-ray diffraction results that the material was $Li_{1.81}H_{0.19}Ti_2O_5{\cdot}xH_2O$. Later it can be observed that the crystal water structure helped to improve the material's lithium ion mobility and to promote its rate capability and cycling stability.

Through N_2 absorption–desorption method, the specific surface areas of hydrogen titanate and lithium titanate hydrate nanotubes were obtained; they were 394.9 $m^2\,g^{-1}$ and 299.3 $m^2\,g^{-1}$, respectively. These values are higher than that of spinel $Li_4Ti_5O_{12}$

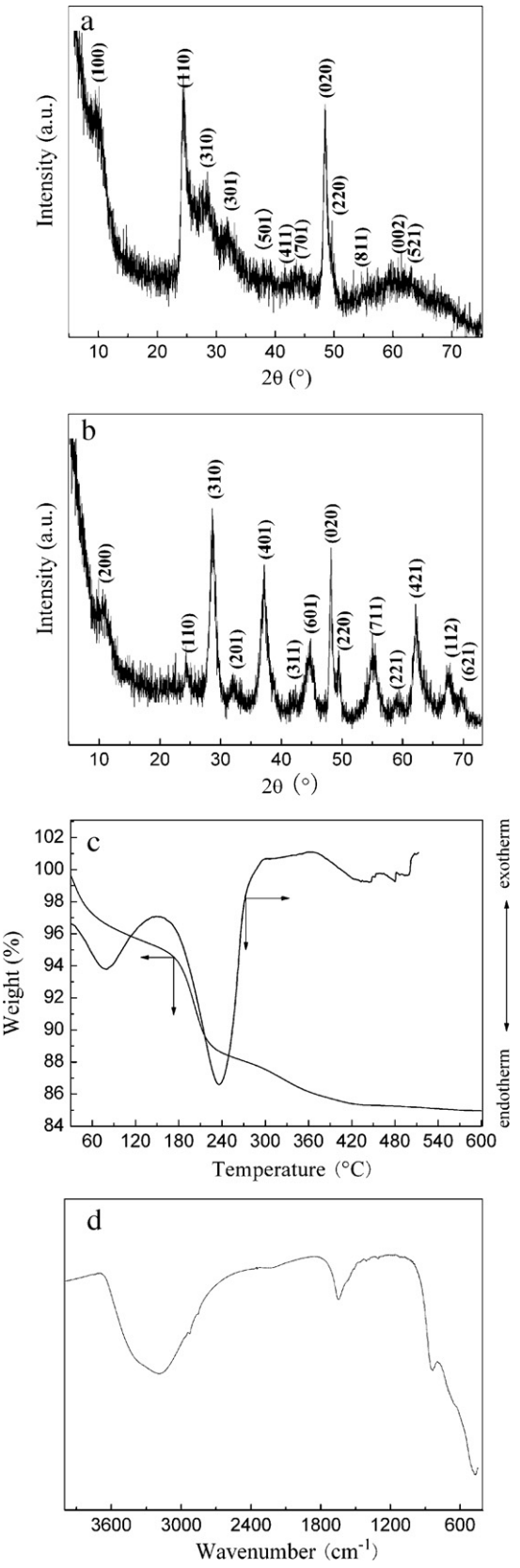

Fig. 2. Characterization of hydrogen titanate precursors and as-prepared lithium titanate hydrate nanotubes. (a and b) Powder X-ray diffraction patterns (using Cu Kα radiation) shows the hydrogen titanate precursors are $H_2Ti_2O_5{\cdot}xH_2O$ and the as-prepared lithium titanate nanotubes are $Li_{1.81}H_{0.19}Ti_2O_5{\cdot}xH_2O$. (c) Thermogravimetric-differential thermal analysis indicates the formula of the material is $Li_{1.81}H_{0.19}Ti_2O_5{\cdot}1.2H_2O$. (d) Infrared spectra pattern, suggesting the possible existence of crystal water in the as-prepared material.

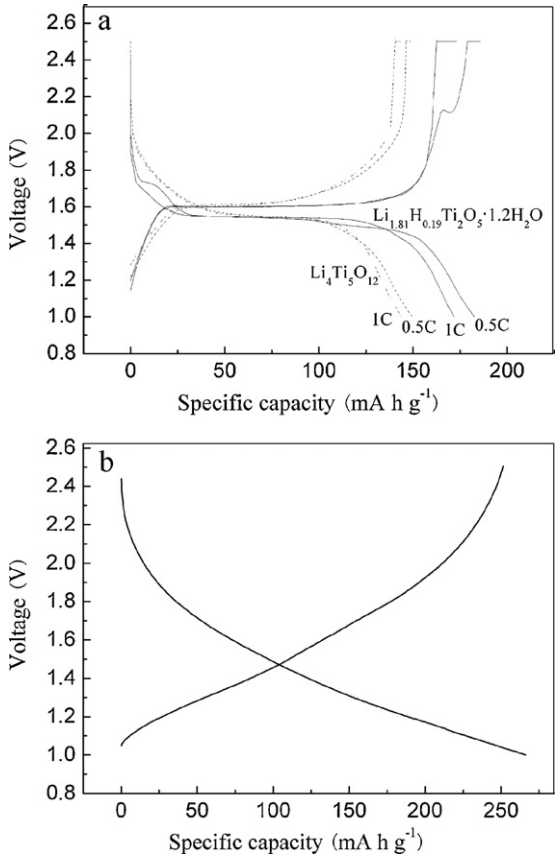

Fig. 3. Charge/discharge voltage profiles of (a) as-prepared lithium titanate and lithium titanate hydrate nanotubes. (b) Hydrogen titanate precursors.

nanotubes [17], resulting from a preparation process free from heat treatment. Nanotube materials with high specific areas have better contacts with electrolytes than conventional powders. Moreover, in these materials the distance that Li^+ ions must diffuse is restricted to the small radius direction of the nanotubes. These two factors contribute to improved lithium ion intercalation efficiency within the electrode material, and hence promote the rate capabilities of the batteries.

3.2. Electrochemical properties by galvanostatic lithium intercalation

Charge/discharge test results show that very high capacities can be achieved with $Li_{1.81}H_{0.19}Ti_2O_5{\cdot}1.2H_2O$ nanotubes. The discharge capacity of $Li_{1.81}H_{0.19}Ti_2O_5{\cdot}1.2H_2O$ nanotubes was 228 mAh g^{-1} (based on the measured weight of the electrode film, including carbon and binder) for the first charge/discharge cycle at a rate of 0.3 C. After several cycles, the capacities of the batteries dropped a little and tended to be stable. Fig. 3a shows the stable charge/discharge voltage profile of $Li_{1.81}H_{0.19}Ti_2O_5{\cdot}1.2H_2O$ and $Li_4Ti_5O_{12}$ nanotubes. It can be noted that the discharge capacities of $Li_4Ti_5O_{12}$ nanotubes at 0.5 C and 1 C were 150 and 145 mAh g^{-1}, respectively, while the corresponding discharge capacities of $Li_{1.81}H_{0.19}Ti_2O_5{\cdot}1.2H_2O$ nanotubes were 181 and 174 mAh g^{-1}, which were approximately 30 mAh g^{-1} higher than those of $Li_4Ti_5O_{12}$ nanotubes. At 0.5 C $Li_{1.81}H_{0.19}Ti_2O_5{\cdot}1.2H_2O$ nanotubes had two pairs of charge/discharge plateaus: a long pair at around 1.5–1.6 V and a small pair at 1.75 V (discharge voltage) and 2.10 V (charge voltage). The occurrence of this extra small pair of plateaus under very low charge/discharge rates is believed to result not from another material mixed with the lithium titanate hydrate,

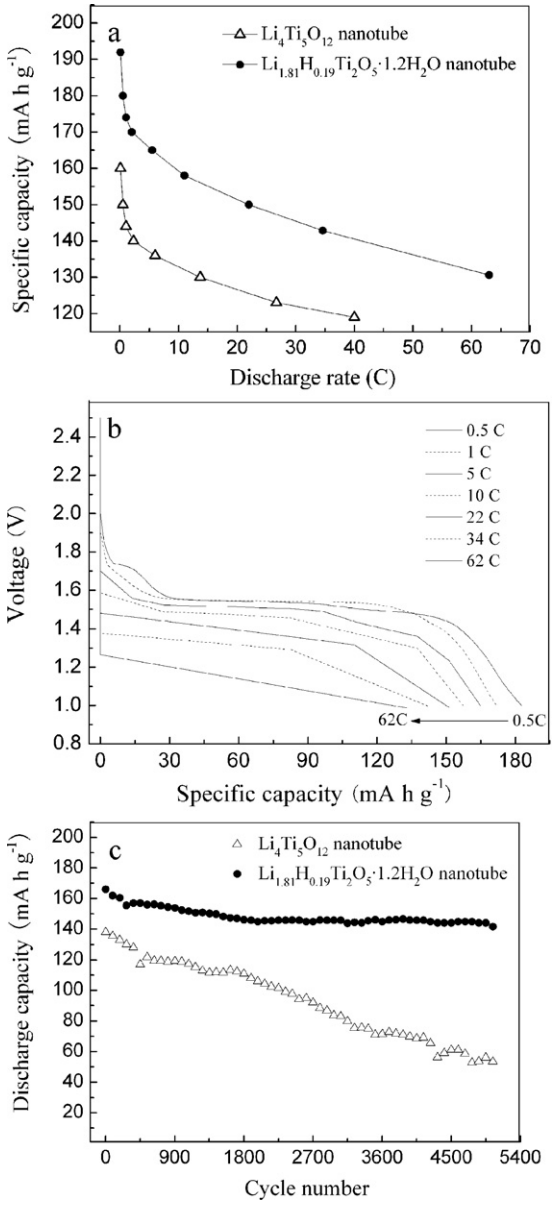

Fig. 4. Electrochemical property comparison of as-prepared lithium titanate and lithium titanate hydrate nanotubes. (a) Discharge capacities of the two samples under various current densities, showing a much larger capacity and a better rate capability of $Li_{1.81}H_{0.19}Ti_2O_5{\cdot}1.2H_2O$ nanotubes. (b) Discharge profiles for $Li_{1.81}H_{0.19}Ti_2O_5{\cdot}1.2H_2O$ nanotubes at various discharge rates. (c) Cycling stabilities of the two samples, indicating $Li_{1.81}H_{0.19}Ti_2O_5{\cdot}1.2H_2O$ nanotubes have even better cycling stabilities than "zero-strain" lithium insertion host spinel $Li_4Ti_5O_{12}$ nanotubes.

but the material itself. The reason that lead to this conclusion is that there were no extra small pair of plateaus under very low charge/discharge rates with hydrogen titanate precursors (as indicated in Fig. 3b) and it is impossible that these extra plateaus result from LiOH impurities. At a higher charge/discharge rate (1 C) after cycles at 0.5 C, the small pair of plateaus disappeared.

$Li_{1.81}H_{0.19}Ti_2O_5{\cdot}1.2H_2O$ nanotubes has superior discharge capacities than $Li_4Ti_5O_{12}$ nanotubes at very high rates too, as indicated in Fig. 4a and b. At 62C (less than 1-min total discharge) the $Li_{1.81}H_{0.19}Ti_2O_5{\cdot}1.2H_2O$ nanotubes could still maintain a discharge capacity as high as 131 mAh g^{-1}. In Fig. 4b, due to fewer recorded data at high charge/discharge rates, the discharge voltage profiles for $Li_{1.81}H_{0.19}Ti_2O_5{\cdot}1.2H_2O$ nanotubes at high rates are broken lines rather than curves.

Fig. 4c shows the cycling stability of $Li_4Ti_5O_{12}$ and $Li_{1.81}H_{0.19}Ti_2O_5{\cdot}1.2H_2O$ nanotubes at a charge/discharge rate of 6 C. An extremely long cycle life can be achieved with lithium titanate hydrate nanotubes. In the first 100 charge/discharge cycles, $Li_4Ti_5O_{12}$ nanotubes, known as the "zero-strain" lithium insertion host, retained a discharge capacity of 136 mAh g^{-1}, and $Li_{1.81}H_{0.19}Ti_2O_5{\cdot}1.2H_2O$ nanotubes retained 162 mAh g^{-1}, both of which were approximately 98% of their initial values. However, $Li_{1.81}H_{0.19}Ti_2O_5{\cdot}1.2H_2O$ nanotubes show much better cycling stability in a longer cycling time. After charge and discharge for 1700 times, $Li_4Ti_5O_{12}$ retained 81% of its initial discharge capacity, while $Li_{1.81}H_{0.19}Ti_2O_5{\cdot}1.2H_2O$ retained 89%. Thereafter the capacity of the former material dropped more intensely, retaining only 38% (53 mAh g^{-1}) after 5000 times of charging/discharging, compared to $Li_{1.81}H_{0.19}Ti_2O_5{\cdot}1.2H_2O$'s 86.3% (143.3 mAh g^{-1}). By comparison, it can be noted that $Li_{1.81}H_{0.19}Ti_2O_5{\cdot}1.2H_2O$ had a longer cycle life than "zero-strain" lithium insertion host $Li_4Ti_5O_{12}$ nanotubes. We believe the outstanding electrochemical properties of $Li_{1.81}H_{0.19}Ti_2O_5{\cdot}1.2H_2O$ nanotubes are owing to intrinsic property of the material, as well as to its containing of crystal water and nanotube structure. The crystal water and nanotube structure help to promote the efficiency of lithium-ion migration. When the crystal water encounters lithium ions, a bond exchange mechanism may occur, similar to proton transfer in water, and this mechanism helps improve the lithium ion transportion which can enhance both the rate capabilities and cycling stabilities of the material. Actually, the low lithium ion mobility of $Li_4Ti_5O_{12}$ greatly limits its cycleability. This is because the efficient distance of the lithium ion can transport is so short because of the low lithium ion mobility that for each cycle after charging, some $Li_{4+x}Ti_5O_{12}$ will be left and could not totally turn into $Li_4Ti_5O_{12}$. This can cause serious capacity decay and poor cycleability. For lithium titanate hydrate nanotubes, the crystal water improves the lithium ion mobility by the possible bond exchange mechanism, and thus not only improved the rate capability of the material but also the cycling stability as well. In addition, the crystal water incorporated in the interlayer of $Li_{1.81}H_{0.19}Ti_2O_5{\cdot}1.2H_2O$ ensures the elasticity of the layer structure [28], which keeps the material from undergoing too much structure change in the process of lithium ion insertion/extraction and promotes lithium ion mobility.

3.3. Kinetics investigation

Fig. 5a presents the AC impedance measurement of $Li_4Ti_5O_{12}$ and $Li_{1.81}H_{0.19}Ti_2O_5{\cdot}1.2H_2O$ nanotubes. It is composed of two semicircles in the medium frequency range and a spike in the low frequency range. The very small semi-circle on the left results from the SEI film on the interface between the cathode and the electrolyte; and the big semi-circle results from the charge-transfer process at the electrode/electrolyte interface. The spike indicates the Warburg impedance of long-range Li-ion diffusion within the cathode. The impedance about Li metal electrode does not appear in Fig. 5a, which may be because it is overlapped with the semi-circles for the cathode. By comparing the charge-transfer resistance of $Li_4Ti_5O_{12}$ with $Li_{1.81}H_{0.19}Ti_2O_5{\cdot}1.2H_2O$ nanotubes, it can be noticed that the resistance of $Li_4Ti_5O_{12}$ nanotubes was larger than that of $Li_{1.81}H_{0.19}Ti_2O_5{\cdot}1.2H_2O$, resulting from the latter material's containing of crystal water and larger surface area. These advantages help $Li_{1.81}H_{0.19}Ti_2O_5{\cdot}1.2H_2O$ to achieve comparatively superior rate capabilities and a longer cycle life.

Fig. 5b shows the cyclic voltammogram profiles of $Li_{1.81}H_{0.19}Ti_2O_5{\cdot}1.2H_2O$ nanotubes at a scan rate of 0.05 mV s^{-1}. It can be observed that lithium titanate hydrate nanotubes had two sharp redox peaks at 1.62 V and 1.50 V, respectively, corresponding with the long charge/discharge plateaus of Fig. 3a, and two small peaks at around 2.00 V and 1.75 V, corresponding

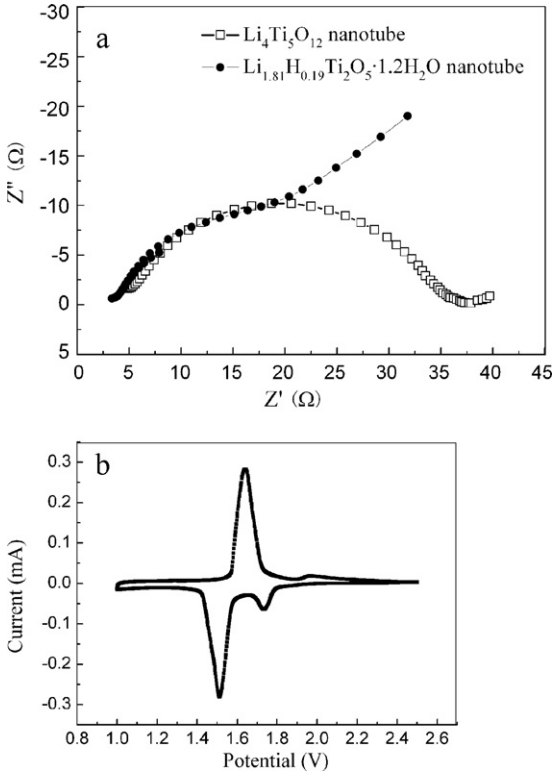

Fig. 5. Electrochemical mechanism studies of as-prepared lithium titanate hydrate nanotubes. (a) AC impedance measurement (1.6 V, 0.1–10^5 Hz). (b) Cyclic voltammogram (2.5–1.0 V, scan rate of 0.05 mV s^{-1}).

with the small pair of plateaus. Materials with similar cyclic voltammogram profiles that contain two pairs of redox peaks have been reported and found to be attractive as electrode materials for lithium batteries [24,32]. Lithium titanate hydrate nanotubes were prepared from their precursor of hydrogen titanate nanotubes, but their charge/discharge voltage profile was very different from the precursors. Hydrogen titanate nanotubes had no plateaus during charging and discharging [28,29], while lithium titanate hydrate nanotubes had two pairs of obvious plateaus (as shown in Fig. 3a and b). Both voltage profiles indicate a pseudocapacitive lithium intercalation mechanism which can promote the rate capability for electrode materials. What makes lithium titanate hydrate a superior material than its hydrogen titanate precursor is that it has charge/discharge plateaus. Battery materials with plateaus while charging and discharging are more suitable for consumer using, as they could function more effectively and more stably within the working voltage range for most electrical devices.

From the data collected by CV measurements and discharge/charge tests, we can assume that the Li^+ ion intercalation into lithium titanate hydrate nanotubes has similar behavior to TiO_2 and $H_2Ti_3O_7$ [29], and can be expressed by Eq. (1):

$$Li_{1.81/2}H_{0.19/2}TiO_{5/2}{\cdot}0.6H_2O + x(Li^+ + e^-) \rightarrow Li_{x+1.81/2}H_{0.19/2}TiO_{5/2}{\cdot}0.6H_2O \quad (0 \geq x \leq 1) \tag{1}$$

when $x = 1$, the specific capacity of $Li_{1.81}H_{0.19}Ti_2O_5{\cdot}1.2H_2O$ nanotubes is 249 mAh g^{-1}. Moreover, from this equation, it can be noticed that there are two different kinds of positions in $Li_{1.81}H_{0.19}Ti_2O_5{\cdot}1.2H_2O$'s crystal lattice for Li^+ ions to intercalate into and de-intercalating from. That is, one position near lithium of $Li_{1.81}H_{0.19}Ti_2O_5$ and another one near hydrogen. Thus it can be speculated that the two pairs of plateaus of lithium titanate hydrate nanotubes during charging/discharging may relate to the different electric potentials of Li^+ ion intercalating/de-intercalating into/out

of the two lattice positions of the material. The long plateaus may correspond to Li^+ intercalating/de-intercalating near lithium in $Li_{1.81}H_{0.19}Ti_2O_5$, while the small plateaus correspond to Li^+ intercalating/de-intercalating near hydrogen in $Li_{1.81}H_{0.19}Ti_2O_5$. This speculation well agrees with the fact that we consistently found 15–20 mAh g^{-1} capacity in the small plateaus (as shown in Fig. 3a), which is around one tenth of the total capacity of the material (181 mAh g^{-1}), and meanwhile the number of hydrogen (0.19) to the total number of hydrogen and lithium (1.9) in $Li_{1.81}H_{0.19}Ti_2O_5$ is also one-tenth. Further characterizations are needed to confirm this speculation.

4. Conclusions

Novel lithium titanate hydrate ($Li_{1.81}H_{0.19}Ti_2O_5{\cdot}1.2H_2O$) nanotubes, on which few reports have been found, were prepared using an economical and uncomplicated method of hydrothermal lithium ion exchange. These nanotubes have demonstrated extraordinary rate capabilities, an extremely long cycle life and much larger reversible capacity than $Li_4Ti_5O_{12}$ nanotubes. The material kept a stable cycling discharge capacities of 181 mAh g^{-1} at 0.5 C (corresponding to a 2-h total discharge) and 131 mAh g^{-1} at 62 C (less than 1-min total discharge). After charge/discharge at 6 C (corresponding to a 10-min total discharge) for 5000 times, this material could still retain 86.3% of its original capacity. These fascinating electrochemical properties indicate that lithium titanate hydrate nanotubes may find promising applications in lithium ion batteries and electrochemical supercapacitors with high energy density and high power density. The abilities of lithium titanate hydrate nanotubes to fully charge within minutes for thousands of times and still retain a large capacity may make a change to people's life.

Acknowledgements

R. Xu thanks F.Y. Kang, L. Zou and X. Fan for the help with electrochemical workstation for cyclic voltammogram measurements and AC impedance measurements. Language revision help from H. Howard is gratefully acknowledged. Support from the Natural Science Foundation of China (no. 50602050) and the National High Technology Research and Development Program of China (863 Program, no. 2007AA03Z235) is gratefully acknowledged.

References

[1] G.H. Du, Q. Chen, R.C. Che, Z.Y. Yuan, L.M. Peng, Appl. Phys. Lett. 79 (2001) 3702–3704.
[2] Y.X. Zhang, G.H. Li, Y.X. Jin, Y. Zhang, J. Zhang, et al., Chem. Phys. Lett. 365 (2002) 300–304.
[3] G.H. Du, Q. Chen, P.D. Han, Y. Yu, L.M. Peng, Phys. Rev. B 67 (2003) 035323.
[4] J. Kim, J. Cho, Electrochem. Solid State Lett. 10 (2007) A81–A84.
[5] T. Ohzuku, A. Ueda, N. Yamamoto, Y. Iwakoshi, J. Power Sources 54 (1995) 99–102.
[6] S.H. Huang, Z.Y. Wen, X.J. Zhu, X.L. Yang, J. Electrochem. Soc. 152 (2005) A1301–A1305.
[7] K. Zaghib, M. Simoneau, M. Armand, M. Gauthier, J. Power Sources 81/82 (1999) 300–305.
[8] A. Guerfi, S. Sevigny, M. Lagace, P. Hovington, K. Kinoshita, et al., J. Power Sources 119 (2003) 88–94.
[9] V.S. Hernandez, L.M.T. Martinez, G.C. Mather, A.R. West, J. Mater. Chem. 6 (1996) 1533–1536.
[10] A. Guerfi, P. Charest, K. Kinoshita, M. Perrier, K. Zaghib, J. Power Sources 126 (2004) 163–168.
[11] S.H. Huang, Z.Y. Wen, X.J. Zhu, Z.H. Gu, Electrochem. Commun. 6 (2004) 1093–1097.
[12] S.H. Huang, Z.Y. Wen, B. Lin, J.D. Han, X.G. Xu, J. Alloys Compd. 457 (2008) 400–403.
[13] D. Wang, H.Y. Xu, M. Gu, C.H. Chen, Electrochem. Commun. 11 (2009) 50–53.
[14] J. Wolfenstine, J.L. Allen, J. Power Sources 180 (2008) 582–585.
[15] H.L. Zhao, Y. Li, Z.M. Zhu, J. Lin, Z.H. Tian, et al., Electrochim. Acta 53 (2008) 7079–7083.
[16] L. Kavan, M. Gratzel, Electrochem. Solid State Lett. 5 (2002) A39–A42.
[17] J.R. Li, Z.L. Tang, Z.T. Zhang, Electrochem. Commun. 7 (2005) 894–899.
[18] J. Wolfenstine, U. Lee, J.L. Allen, J. Power Sources 154 (2006) 287–289.
[19] T. Kasuga, M. Hiramatsu, A. Hoson, T. Sekino, K. Niihara, Adv. Mater. 11 (1999) 1307–1311.
[20] Q. Chen, W.Z. Zhou, G.H. Du, L.M. Peng, Adv. Mater. 14 (2002) 1208–1211.
[21] S. Zhang, L.M. Peng, Q. Chen, G.H. Du, G. Dawson, et al., Phys. Rev. Lett. 91 (2003) 256103.
[22] J.R. Li, Z.L. Tang, Z.T. Zhang, Electrochem. Commun. 7 (2005) 62–67.
[23] J.J. Yang, Z.S. Jin, X.D. Wang, W. Li, J.W. Zhang, et al., Dalton Trans. 20 (2003) 3898–3901.
[24] A.R. Armstrong, G. Armstrong, J. Canales, P.G. Bruce, Angew. Chem. 43 (2004) 2286–2288.
[25] R. Ma, Y. Bando, T. Sasaki, Chem. Phys. Lett. 380 (2003) 577–582.
[26] J.P. Zheng, T.R. Jow, J. Electrochem. Soc. 145 (1998) 49–52.
[27] M. Tsuda, H. Arai, Y. Sakurai, J. Power Sources 110 (2002) 52–56.
[28] S. Bach, J.P. Pereira-Ramos, N. Baffier, J. Electrochem. Soc. 143 (1996) 3429–3434.
[29] J.R. Li, Z.L. Tang, Z.T. Zhang, Chem. Mater. 17 (2005) 5848–5855.
[30] Q. Chen, G.H. Du, S. Zhang, L.M. Peng, Acta Crystallogr. 58 (2002) 587–593.
[31] J. Li, Y.L. Jin, X.G. Zhang, H. Yang, Solid State Ionics 178 (2007) 1590–1594.
[32] S.K. Martha, J. Grinblat, O. Haik, E. Zinigrad, et al., Angew. Chem. Int. Ed. 48 (2009) 8559–8563.